Organic Chemistry
Current Research
ISSN: 2161-0401

Jin, Organic Chem Curr Res 2015, 4:1
DOI: 10.4172/2161-0401.1000134

Research Article Open Access

Rational Design of Star-Shaped Molecules with Benzene Core and Naphthalimides Derivatives End Groups as Organic Light-emitting Materials

Ruifa Jin*

College of Chemistry and Chemical Engineering, Chifeng University, Chifeng 024000, China

Abstract

A series of star-shaped molecules with benzene core and naphthalimides derivatives end groups have been designed to explore their optical, electronic, and charge transport properties as charge transport and/or luminescent materials for organic light-emitting diodes (OLEDs). The frontier molecular orbitals (FMOs) analysis has turned out that the vertical electronic transitions of absorption and emission are characterized as intramolecular charge transfer (ICT). The calculated results show that the optical and electronic properties of star-shaped molecules are affected by the substituent groups in N-position of 1,8-naphthalimide ring. Our results suggest that star-shaped molecules with n-butyl (**1**), Benzene (**2**), Thiophene (**3**), thiophene *S'*,*S'*-dioxide (**4**), benzo[c][1,2,5]thiadiazole (**5**), and 2,7a-dihydrobenzo[d] thiazole (**6**) fragments are expected to be promising candidates for luminescent and electron transport materials for OLEDs. This study should be helpful in further theoretical investigations on such kind of systems and also to the experimental study for charge transport and/or luminescent materials for OLEDs.

Keywords: 1,8-Naphthalimide derivatives; Optical and electronic properties; Charge transport property; Luminescent materials; Organic light-emitting diodes (OLEDs)

Introduction

Organic light-emitting diodes (OLEDs) have received considerable interest due to their promising applications in the large-area flat-panel displays and solid-state lighting [1-6]. The devices using organic materials have shown several advantages over their inorganic counterparts, for example, light weight, potentially low cost, capability of thin-film, large-area, and flexible device fabrication, and wide selection of emission colors via molecular design of organic materials. However, the lower efficiency of OLEDs is a thorny obstacle to the application of efficient light-emitting devices. Since the first report on OLEDs in 1987, the light generation efficiencies of OLEDs have been steadily increased by using novel materials and the different device structures [7-9]. Unfortunately, most OLEDs emitters are still not satisfactory. Therefore, the design and synthesize for new emitting materials with high efficiency and thermal stability remain one of the most active areas of the studies. A number of studies demonstrate that the interplay between theory and experiment is capable of providing useful insights into the understanding of the the nature of molecules [10,11]. Among the various kinds of OLEDs materials, 1,8-naphthalimide (**NI**) derivatives usually exhibit strong fluorescence and good photostability [12-14]. They have been widely used as the most important materials for fabrication of OLEDs. Furthermore, **NI** derivatives have high electron affinity and excellent transport property due to the existence of an electron-deficient centre. Thus, **NI** derivatives have been extensively applied in many fields such as coloration and brightening of polymers [15], potential photosensitive biologically units [16], fluorescent markers in biology [17], light emitting diodes [18,19], fluorescence sensors and switchers [20], and electroluminescent materials [21]. A large variety of auxochromic groups in **NI** derivatives may be easily grafted to fine tune the absorption and emission wavelengths. Naphthalimides comprise a class of fluorophore whose electronic absorption and emission depend upon the properties of the surrounding medium. The emission spectrum can be tuned by introducing different electron-donating substituent groups, such as N-substituted groups [22], C-substituted groups [23], and O-substituted groups [24]. Furthermore, substitution of electron-donating groups usually increases the intensity of the fluorescence emission, particularly when a methoxy or amino group at C-4 position is used. Recently, some starburst amorphous molecules 1,3,5-Tris(1,8-naphthalimide-4-yl)benzenes have been reported [25]. It was found that the devices using these molecules performance are better than using the most prevalent tris(8-quinolinato)aluminum (Alq3) as a counterpart.

With the above considerations, in this work, we investigated a series of star-shaped molecules with benzene as core and **NI** derivatives as end groups for OLEDs applications (Scheme 1). An in-depth interpretation of the optical and electronic properties of these compounds has been presented. Several derivatives (**1**–**6**), as shown in Scheme 1, have been designed to provide a demonstration for the rational design of novel luminescent and charge transporting materials for OLEDs (Scheme 1).

Computational Methods

All calculations have been performed using Gaussian 09 code [26]. Generally, the B3LYP method appeared notably adapted to **NI** derivatives [27-31]. Therefore, The geometry optimization of designed molecules in ground states (S_0) were carried out by the B3LYP method using the 6-31G(d,p) basis set. The corresponding geometry in the first excited singlet state (S_1) were optimized using the TD-B3LYP with 6-31G (d,p) basis set. The harmonic vibrational frequency calculations using the same methods as for the geometry optimizations were used to ascertain the presence of a local minimum. The absorption and fluorescent properties of **1**–**6** have been predicted using the TD-B3LYP/6-31G(d,p) method based on the S_0 and S_1 optimized geometries, respectively. To investigate the influence of solvents on the optical properties for the S_0 and S_1 states of the molecular systems

***Corresponding author:** Ruifa Jin, College of Chemistry and Chemical Engineering, Chifeng University, Chifeng 024000, China, Tel: 86-0476-8300370; E-mail: Ruifajin@163.com

Received: October 06, 2014; **Accepted:** January 13, 2015; **Published**: January 17, 2015

Citation: Jin R (2015) Rational Design of Star-Shaped Molecules with Benzene Core and Naphthalimides Derivatives End Groups as Organic Light-emitting Materials. Organic Chem Curr Res 4:134. doi:10.4172/2161-0401.1000134

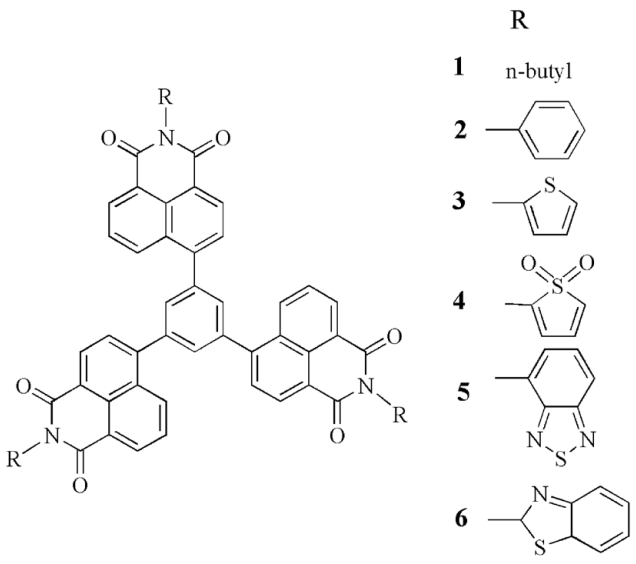

Scheme 1: Geometries of Designed Molecules 1–6.

in chloroform (dielectric constant: 2.0906) solvent, we performed the polarized continuum model (PCM) [32] calculations at the TD-DFT level.

The stability is a useful criterion to evaluate the nature of devices for charge transport and luminescent materials. To predict the stability of **1**–**6** from a viewpoint of conceptual density functional theory, the absolute hardness, η, of **1**–**6** were calculated using operational definitions [33,34] given by:

$$\eta = \frac{1}{2}\left(\frac{\partial \mu}{\partial N}\right) = \frac{1}{2}\left(\frac{\partial^2 E}{\partial N^2}\right) = \frac{IP - EA}{2} \quad (1)$$

Where, μ is the chemical potential and N is the total electron number. In this work, the values for IP (ionization potential) and EA (electron affinity) were determined according to the equation $IP = E_{cr} - E_p$ and $EA = E_p - E_{ar}$, where p, cr, and ar indicate the parent molecule and the corresponding cation and anion radical generated after electron transfer.

Results and Discussion

Frontier molecular orbitals

To characterize the optical transitions and the abilities of electron and hole transport, it is useful to examine the frontier molecular orbitals (FMOs) of the compounds under investigation. The origin of the geometric difference introduced by excitation can be explained, at least in qualitative terms, by analyzing the change in the bonding character of the orbitals involved in the electronic transition for each pair of bonded atoms. An electronic excitation results in some electron density redistribution that affects the molecular geometry [35]. We calculated the distribution patterns of FMOs for **1**–**6** in S_0 (Figure 1). The total and partial densities of states (TDOS and PDOS) on each fragment of the investigated molecules around the HOMO – LUMO gaps were calculated based on the current level of theory. The FMOs energies E_{HOMO} and E_{LUMO}, HOMO – LUMO gaps, and the contributions of individual fragments (in %) to the FMOs of **1**–**6** are given in Table 1. As shown in Figure 1, the $S_0 \rightarrow S_1$ excitation process can be mainly assigned to the HOMOs → LUMOs and HOMOs-1 → LUMOs transitions, which correspond to a π–π^* excited singlet state. For **1**, **2**, and **5**, the HOMOs are distributed on the 1,8-naphthalimide (**NI**) and benzene (**BZ**) moieties, with minor contributions from N-substituent groups (**SG**). The sum contributions of **NI** and **BZ** fragments of HOMOs are larger than 97.2%, while the corresponding contributions of **SG** fragments are within 2.8%, respectively. For **3** and **6**, the HOMOs are mainly localized on the **SG** fragments with only minor contributions from **NI** and **BZ** fragments. The contributions of **SG** fragments of HOMOs are larger than 95%, while the corresponding sum contributions of **NI** and **BZ** fragments are within 4.9%, respectively. For **4**, the HOMOs are distributed on the **NI** and **SG** fragments, with minor contributions from **BZ** fragment. However, the LUMOs of **1**–**6** are mainly composed

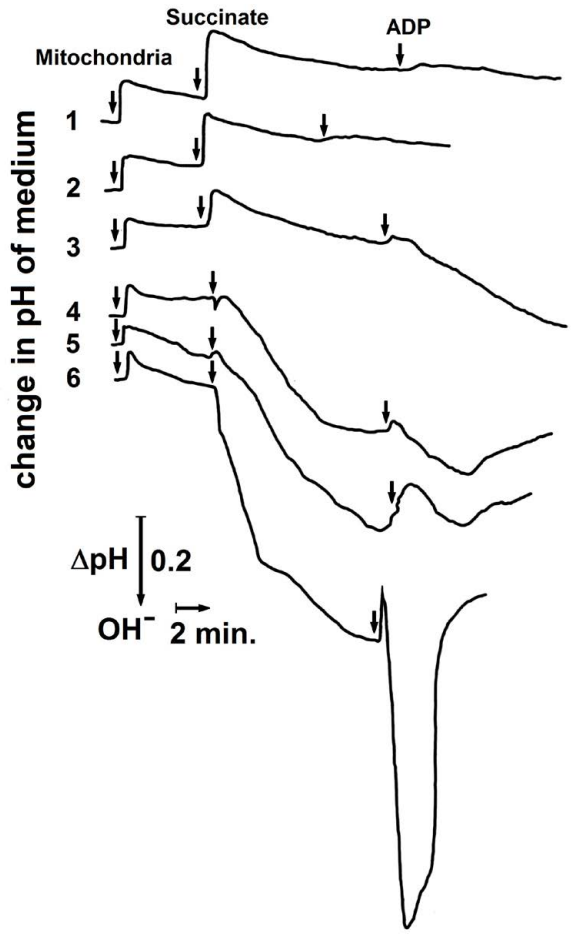

Figure 1: Electronic density contours of the frontier molecular orbitals for investigated derivatives.

	HOMO				LUMO				
Species	E_{HOMO}	NI[a]	BZ[b]	SG[c]	E_{LUMO}	NI	BZ	SG	E_g
1	-6.54	85.5	14.4	0.1	-2.69	92.7	7.3	0.0	3.85
2	-6.54	84.4	14.2	1.4	-2.69	92.6	7.4	0.0	3.85
3	-6.41	4.9	0.0	95.1	-2.77	93.0	7.0	0.0	3.64
4	-6.81	53.6	8.5	37.9	-3.02	92.8	6.9	0.2	3.79
5	-6.59	83.8	13.4	2.8	-2.74	92.9	6.9	0.2	3.85
6	-6.44	1.9	0.1	98.1	-2.87	92.9	7.1	0.0	3.57

[a] NI: 1,8-naphthalimide moieties; [b] BZ: benzene moieties; [c] SG: substituent groups

Table1: The FMOs Energies E_{HOMO} and E_{LUMO}, HOMO–LUMO gaps (eV), and HOMOs and LUMOs Contributions (%) of 1–6.

Species	λ_{ab}	*f*	Assignment
1	365	0.85	HOMO-1 → LUMO (0.70) HOMO-1 → LUMO+2 (0.12)
2	365	0.62	HOMO → LUMO (-0.31) HOMO → LUMO+1 (-0.32) HOMO-1 → LUMO (0.43)
3	365	0.52	HOMO → LUMO (0.60) HOMO → LUMO+2 (0.14)
4	370	0.60	HOMO → LUMO (0.59) HOMO → LUMO+2 (0.12)
5	365	0.57	HOMO → LUMO (0.58) HOMO → LUMO+1 (0.17)
6	368	0.59	HOMO → LUMO (0.45) HOMO → LUMO+1 (0.20) HOMO → LUMO+2 (0.22)
Exp[a]	360		

[a] Experimental data for **1** in chloroform [25].

Table 2: The absorption wavelengths λ_{abs} (in nm), the oscillator strength *f*, and main assignments (coefficient) of 1–6 in chloroform obtained at the TD-B3LYP/6-31G(d,p)//B3LYP/6-31G(d,p) level, along with available experimental data.

of contributions of **NI**, with minor contributions from **SG** and **BZ** fragments. The contributions of **NI** fragments of LUMOs are larger than 92.6%, while the corresponding sum contributions of **SG** and **BZ** fragments are within 7.4%, respectively.

The distribution patterns of the FMOs also provide a remarkable signature for the charge-transfer character of the vertical $S_0 \rightarrow S_1$ transition. Analysis of the FMOs indicates that the excitation of the electron from the HOMO to LUMO leads the electronic density to flow mainly from the **SG** and **BZ** fragments to **NI** fragments for **1, 2, 4**, and **5**. The percentages of charge transfer are the differences between the contributions of fragments for LUMOs and the corresponding contributions for HOMOs in the compounds under investigation. The percentages of charge transfer from **SG** and **BZ** fragments to **NI** fragments are 7.2, 8.2, 39.2, and 9.1%, respectively. On the contrary, for **3** and **6**, the excitation of the electron from the HOMO to LUMO leads the electronic density to flow mainly from **SG** fragments to **BZ** and **NI** fragments. The percentage of charge transfer of 3 and **6** are 95.1 and 98.1%, respectively.

Another way to understand the influence of the optical and electronic properties is to analyze the E_{HOMO}, E_{LUMO}, and E_g values. From Table 1, one can find that the E_{HOMO} values of **2**, **4**, and **5** decreases, while the corresponding value of **3** and **6** increase compared with that of **1**. The HOMOs energies are in the order of **3** > **6** > **1** ≈ **2** > **5** **4**. However, the values of E_{LUMO} and HOMO–LUMO gaps E_g for **2**–**6** decrease compared with those of **1**. The sequence of LUMOs energies is **1** ≈ **2** ≈ **5** > **3** **6** > **4**. The E_g values are in the order of **1** ≈ **2** ≈ **5** > **4** **3** > **6**. It implies that the introduction of different donor groups to the **1** leads to the change of the E_{HOMO}, E_{LUMO}, and E_g values for its derivatives. The absorption and fluorescence spectra can be tuned by donor groups, providing a powerful strategy for prediction of the optical properties of novel electroluminophores.

Absorption and Fluorescence Spectra

The absorption λ_{abs} and fluorescence λ_{fl} wavelengths, main assignments, and the oscillator strength *f* for the most relevant singlet excited states in each molecule are listed in Tables 2 and 3, respectively. The λ_{abs} and λ_{fl} values of **1** are all in agreement with experimental results [25], the deviations are 5 and 25 nm, respectively. The Stokes shift of **1** is 36 nm, which is comparable to the experimental 66 nm. Thus, this result credits to the computational approach, so appropriate electronic transition energies can be predicted at these levels for this kind of system.

For the absorption spectra, the excitation to the S_1 state corresponds mainly to the HOMO-1 → LUMO for **1**, while the corresponding excitations for **2**–**6** correspond mainly to the HOMOs → LUMOs and HOMOs → LUMOs+1 and/or HOMOs → LUMOs + 2. From Table 2, one can find that the λ_{abs} values of **1**–**6** are almost equal to that of **1**. It suggests that the substituent effects do not significantly affect the absorption spectra of **2**–**6** compared with those of **1**. Moreover, **2**–**6** have nearly equal values of oscillator strengths, being smaller slightly than the value of **1**. The oscillator strength for an electronic transition is proportional to the transition moment [36]. In general, larger oscillator strength corresponds to larger experimental absorption coefficient or stronger fluorescence intensity. This implies that these bipolar molecules shown large absorption intensity.

For the fluorescence spectra, the HOMO ← LUMO+1 and HOMO-1 ← LUMO excitations play a dominant role for **1**. The fluorescence peaks of **2**, **3**, and **5** are mainly correspond to HOMOs-1 ← LUMOs excitations. The λ_{fl} value of **2** is almost equal to that of **1**, while the λ_{fl} values of **3**–**6** show bathochromic shifts 5, 27, 8, and 53 nm compared with that of **1**, respectively. The Stokes shifts of **3**–**6** are 41, 58, 44, and 86 nm, respectively. Furthermore, the *f* values **2**–**6** are almost equal to that of **MEBN**, corresponding to strong fluorescence spectra. This implies that **2**–**6** have large fluorescent intensity and they are promising luminescent materials for OLEDs. As shown in Table 3, it clearly shows that the substituent groups can affect the fluorescence spectra of these molecules. The emissions color of molecules can be tuned by the N-substituent groups. Furthermore, all the substituted derivatives show stronger fluorescence intensity (Tables 2 and 3).

Species	λ_{flu}	*f*	Assignment
1	401	0.76	HOMO ← LUMO+1 (0.55) HOMO-1 ← LUMO (-0.43)
2	399	0.83	HOMO ← LUMO+1 (-0.49) HOMO-1 ← LUMO (0.49)
3	406	0.52	HOMO-1 ← LUMO (0.67) HOMO-2 ← LUMO (0.14)
4	428	0.59	HOMO ← LUMO+4 (0.47) HOMO ← LUMO+3 (0.34)
5	409	0.70	HOMO ← LUMO+5 (0.56) HOMO-1 ← LUMO (-0.40)
6	454	0.50	HOMO ← LUMO+1 (-0.41) HOMO-1 ← LUMO (0.67)
Exp[a]	426		

[a] Experimental data for **1** in chloroform [25].

Table 3: The fluorescence wavelengths λ_{flu} (in nm), the oscillator strength *f*, and main assignments (coefficient) of 1–6 in chloroform obtained at the TD-B3LYP/6-31G(d,p)//TD-B3LYP/6-31G(d,p) level, along with available experimental data.

Species	λ_h	λ_e	
1	0.142	0.150	2.827
2	0.328	0.180	2.837
3	0.292	0.156	2.790
4	0.315	0.216	2.670
5	0.304	0.110	2.893
6	0.294	0.122	2.866

Table 4: Calculated molecular λ_e, λ_h, and η (all in eV) of 1–6 at the B3LYP/6-31G(d,p) level.

Charge Transport Properties

The charge transfer rate can be described by Marcus theory [37,38] via the following equation:

$$K = (V^2/\hbar)\left(\pi/\lambda k_B T\right)^{1/2} \exp\left(-\lambda/4k_B T\right) \quad (2)$$

Where, T is the temperature, k_B is the Boltzmann constant, λ represents the reorganization energy due to geometric relaxation accompanying charge transfer, and V is the electronic coupling matrix element (transfer integral) between the two adjacent species dictated largely by orbital overlap. It is clear that two key parameters are the reorganization energy and electronic coupling matrix element, which have a dominant impact on the charge transfer rate, especially the former.

For the reorganization energy λ, they can be divided into two parts, external reorganization energy (λ_{ext}) and internal reorganization energy (λ_{int}). λ_{ext} represents the effect of polarized medium on charge transfer, which is quite complicated to evaluate at this stage. λ_{int} is a measure of structural change between ionic and neutral states [39,40]. Our designed molecules are used as charge transport materials for OLEDs in the solid film; the dielectric constant of the medium for the molecules is low. The computed values of the external reorganization energy in pure organic condensed phases are not only small but also are much smaller than their internal counterparts [41,42]. Moreover, there is a clear correlation between λ_{int} and charge transfer rate in literature [43,44]. Therefore, we mainly study the λ_{int} of the isolated active organic π-conjugated systems owing to ignoring the environmental changes and relaxation in this work. Hence, the λ_e and λ_h can be defined by equations (3) and (4): [45]

$$\lambda_e = \left(E_0^- - E_-^-\right) + \left(E_-^0 - E_0^0\right) \quad (3)$$

$$\lambda_h = \left(E_0^+ - E_+^+\right) + \left(E_+^0 - E_0^0\right) \quad (4)$$

Where, E_0^+ (E_0^-) is the energy of the cation (anion) calculated with the optimized structure of the neutral molecule. Similarly, E_+^+ (E_-^-) is the energy of the cation (anion) calculated with the optimized cation (anion) structure, E_+^0 (E_-^0) is the energy of the neutral molecule calculated at the cationic (anionic) state. Finally, E_0^0 is the energy of the neutral molecule in ground state. For comparing with the interested results reported previously [46,47], the reorganization energies for electron (λ_e) and hole (λ_h) of the molecules were calculated at the B3LYP/6-31G (d,p) level on the basis of the single point energy.

The calculated reorganization energies for hole and electron are listed in Table 4. It is well-known that, the lower the reorganization energy values, the higher the charge transfer rate [37,38]. The results displayed in Table 4 show that the calculated λ_e values of **1**–**6** (0.110 – 0.180 eV) are larger than that of tris(8-hydroxyquinolinato) aluminum(III) (Alq3) (λ_e = 0.276 eV), a typical electron transport material [46]. It indicates that their electron transfer rates might be higher than that of Alq3, suggesting that **1**–**6** could be good electron transfer materials from the stand point of the λ_e values. On the other hand, the calculated λ_h values of **2**–**6** (0.292 – 0.328 eV) are larger than that of N,N'-diphenyl-N,N'-bis(3- methylphenyl)-(1,1'-biphenyl)-4,4'-diamine (TPD), which is a typical hole transport material (λ_h = 0.290 eV) [47]. It indicates that their whole transfer rates might be lower than that of TPD. It indicates that **1**–**6** can be used as promising electron transport materials in OLEDs from the stand point of the smaller reorganization energy.

As the stability is a useful criterion to evaluate the nature of devices for charge transport and luminescent materials. The absolute hardness η is the resistance of the chemical potential to change in the number of electrons. As expected, inspection of Table 4 reveals clearly that the η values of **2**–**6** are almost equal to that of values of **1**. These results reveal that the different π-conjugated bridges do not significantly affect the stability of these bipolar molecules.

Conclusions

In this paper, a series of star-shaped molecules with benzene core and naphthalimides derivatives end groups have been systematically investigated. The FMOs analysis have turned out that the vertical electronic transitions of absorption and emission are characterized as intramolecular charge transfer (ICT). The calculated results show that their optical and electronic properties are affected by their substituent groups in N-position of 1,8-naphthalimide. The study of substituent effects suggest that the λ_{abs} values of **2**–**6** are almost equal to that of the parent compound **1**, while the λ_{fl} of **2**–**6** show bathochromic shifts compared with that of **1**. Furthermore, **2**–**6** have large fluorescent intensity. The different substituent groups do not significantly affect the stability of these molecules. Our results suggest that **2**–**6** are expected to be promising candidates for luminescent materials and electron transport materials for OLEDs.

Acknowledgement

Financial support from the Inner Mongolia Key Laboratory of Photoelectric Functional Materials and Natural Science Foundation of Inner Mongolia Autonomous Region (No. 2011ZD02) are gratefully acknowledged.

References

1. Mullen K, Scherf U (2006) Organic light-emitting devices, synthesis, properties, and applications, Wiley-VCH , Weinheim C.
2. Grimsdale AC , Chan KL, Martin RE, Jokisz PG, Holmes AB (2009) Synthesis of light-emitting conjugated polymers for applications in electroluminescent devices. Chem Rev 109: 897-1091.
3. Minaev B, Baryshnikov G, Agren H (2014) Principles of phosphorescent organic light emitting devices. Phys Chem Chem Phys 16: 1719-1758.
4. Sasabe H , Kido J (2013) Development of high performance OLEDs for general lighting. J Mater Chem 1: 1699-1707.
5. Dimitrakopoulos CD, Malenfant PRL (2002) Organic thin film transistors for large area electronics. Adv Mater 14: 99-117.
6. Yao JH, Zhen C, Loh KP, Chen ZK (2008) Novel iridium complexes as high-efficiency yellow and red phosphorescent light emitters for organic light-emitting diodes. Tetrahedron 64: 10814-1082.
7. Tang CW, VanSlyke SA (1987) Organic electroluminescent diodes. Appl Phys Lett 51: 913-915.
8. Walzer K, Maennig B, Pfeiffer M, Leo K (2007) Highly efficient organic devices based on electrically doped transport layers. Chem Rev 107: 1233-1271.
9. Koh TW, Choi JM, Lee S, Yoo S (2010) Optical out coupling enhancement in organic light-emitting diodes: highly conductive polymer as a low-index layer on micro structured ITO electrodes. Adv Mater 22 : 1849-1853.
10. Liu YL, Feng JK, Ren AM (2008) Theoretical study on photophysical properties of bis-dipolar diphenylamino-endcapped oligoarylfluorenes as light-emitting materials. J Phys Chem A 112: 3157-3164.

11. Zou LY, Ren AM, Feng JK, Liu YL, Ran XQ, et al. (2008) Theoretical study on photophysical properties of multifunctional electroluminescent molecules with different pi-conjugated bridges. J Phys Chem A 112: 12172-12178.

12. Ramachandram B, Saroja G, Sankaran NB, Samanta A (2000) Unusually high fluorescence enhancement of some 1,8-naphthalimide derivatives induced by transition metal salts. J Phys Chem B 104: 11824-11832.

13. Ivanov IP, Dimitrova MB, Tasheva DN, Cheshmedzhieva DV, et al. (2013) Synthesis, structural analysis and application of a series of solid-state fluorochromes-aryl hydrazones of 4-hydrazino-N-hexyl-1,8-naphthalimide. Tetrahedron 69: 712-721.

14. Li Y, Xu Y, Qian X , Qu B (2004) Naphthalimide-thiazoles as novel photonucleases: molecular design, synthesis, and evaluation. Tetrahedron Lett 45: 1247-1251.

15. Hrdlovi P, Chmela S, Danko M, Sarakha M, Guyot G (2008) Spectral properties of probes containing benzothioxanthene chromophore linked with hindered amine in solution and in polymer matrices. J. Fluoresc 18: 393-402.

16. Tao ZF, Qian X (1999) Naphthalimide hydroperoxides as photonucleases: substituent effects and structural basis. Dyes Pigm 43: 139-145.

17. Martin E, Weigand R, Pardo A (1996) Solvent dependence of the inhibition of intramolecular charge-transfer in N-substituted 1,8-naphthalimide derivatives as dye lasers. J Lumin 68: 157-164.

18. Grabchev I, Chovelon JM, Qian X (2003) A copolymer of 4-N,N dimethylaminoethylene-N-allyl-1,8-naphthalimide with methylmethacrylate as a selective fluorescent chemosensor in homogeneous systems for metal cations. J Photochem Photobiol A158: 37-43

19. Morgado J, Gruner J, Walcott SP, Yong TM, Cervini R, et al. (1998) 4-AcNI—a new polymer for light-emitting diodes. Synth Met 95: 113-117.

20. Tamanini E1, Katewa A, Sedger LM, Todd MH, Watkinson M (2009) A synthetically simple, click-generated cyclam-based zinc(II) sensor. See comment in PubMed Commons below Inorg Chem 48: 319-324.

21. Chatterjee S, Pramanik S, Hossain SU, Bhattacharya S, Bhattacharya SC (2007) Synthesis and photoinduced intramolecular charge transfer of N-substituted 1,8-naphthalimide derivatives in homogeneous solvents and in presence of reduced glutathione. J Photochem Photobiol A 187: 64-71.

22. Islam A, Cheng CC, Chi SH, Lee SJ, Hela GP, et al.(2005) Amino naphthalic anhydrides as red-emitting materials:? Electro luminescence, crystal structure, and photo physical properties. J Phys Chem B 109: 5509-5517.

23. Yang JX, Wang XL, Wang XM, Xu LH (2005) The synthesis and spectral properties of novel 4-phenylacetylene-1,8-naphthalimide derivatives. Dyes Pigm 66 : 83-87.

24. Magalhaes JL, Pereira RV, Triboni ER, Berci Filho P, Gehlen MH, et al. (2006) Solvent effect on the photo physical properties of 4-phenoxy-N-methyl-1,8-naphthalimide. J Photochem Photobiol A 183: 165-170.

25. Liu Y, Niu F, Lian J, Zeng P, Niu H (2010) Synthesis and properties of starburst amorphous molecules: 1,3,5-Tris(1,8-naphthalimide-4-yl)benzenes. Synthetic Met 160 : 2055-2060.

26. Frisch MJT, Trucks GW, Schlegel HB, Scuseria GE, Robb MA, et al. (2009) Gaussian 09; Gaussian Inc. Wallingford CT, USA

27. Mancini G, Zazza C, Aschib M, Sannaa N (2011) Conformational analysis and UV/Vis spectroscopic properties of a rotaxane-based molecular machine in acetonitrile dilute solution: when simulations meet experiments. Phys Chem Chem Phys 13: 2342-2349.

28. Li H, Li N, Sun R, Gu H, Ge J, et al. (2011) Dynamic random access memory devices based on functionalized copolymers with pendant hydrazine naphthalimide group. J Phys Chem C 115 : 8288-8294.

29. Dhar S, Roy SS, Rana DK, Bhattacharya S, Bhattacharya S, et al. (2011) Tunable solvatochromic response of newly synthesized antioxidative naphthalimide derivatives: intramolecular charge transfer associated with hydrogen bonding effect. J Phys Chem A 115: 2216-2224.

30. Meng X, Zhu W, Zhang Q, Feng Y, Tan W, et al. (2008) Novel bisthienylethenes containing naphthalimide as the venter ethene bridge: photochromism and solvatochromism for combined NOR and INHIBIT logic gates. J Phys Chem B 112: 15636-15645.

31. Li Z, Yang Q, Chang R, Ma G, Chen M, et al. (2011) N-Heteroaryl-1,8-naphthalimide fluorescent sensor for water: Molecular design, synthesis and proper. Dyes Pigm 88: 307-314.

32. Gudeika D, Michaleviciute A, Grazulevicius JV, Lygaitis R, Grigalevicius S, et al. (2012) Structure properties relationship of donor-acceptor derivatives of triphenylamine and 1,8-naphthalimide. J Phys Chem C 116: 14811-14819.

33. Pearson RG (1985) Absolute electronegativity and absolute hardness of Lewis acids and bases. J Am Chem Soc107: 6801-6806.

34. Stark MS (1997) Epoxidation of alkenes by peroxyl radicals in the gas phase:? structure? activity relationships. J Phys Chem A 101: 8296-8301.

35. Fores M, Duran M, Sola M, Adamowicz L (1999) Excited-state intramolecular proton transfer and rotamerism of 2-(2'-hydroxyvinyl)benzimidazole and 2-(2'-hydroxyphenyl)imidazole. J Phys Chem A 103: 4413-4420.

36. Schleyer P, Von R, Allinger NL, Clark T, Gasteiger J, et al. (1998) Chichester UK.

37. Marcus RA (1993) Electron transfer reactions in chemistry theory and experiment. Rev Mod Phys 65: 599-610.

38. Marcus RA (1964) Chemical and electrochemical electron-transfer theory. Annu Rev Phys Chem 15: 155-196.

39. Lemaur V, Steel M, Beljonne D, Bredas JL, Cornil J (2005) Photoinduced charge generation and recombination dynamics in model donor /acceptor pairs for organic solar cell applications:? a full quantum-chemical treatment. J Am Chem Soc 127: 6077-6076.

40. Hutchison GR1, Ratner MA, Marks TJ (2005) Hopping transport in conductive heterocyclic oligomers: reorganization energies and substituent effects. See comment in PubMed Commons below J Am Chem Soc 127: 2339-2350.

41. Martinelli NG, Ide J, Sánchez-Carrera RS, Coropceanu V, Bredas JL, et al. (2010) Influence of structural dynamics on polarization energies in anthracene single crystals. J Phys Chem C 114: 20678-20685.

42. McMahon DP, Trois A (2010) Evaluation of the external reorganization energy of polyacenes. J Phys Chem Lett 1: 941-946.

43. Köse ME1, Long H, Kim K, Graf P, Ginley D (2010) Charge transport simulations in conjugated dendrimers. J Phys Chem A 114: 4388-4393.

44. Sakanoue K, Motoda M, Sugimoto M, Sakaki S (1999) A molecular orbital study on the hole transport property of organic amine compounds. J Phys Chem A 103: 5551-5556.

45. Köse ME, Mitchell WJ, Kopidakis N, Chang CH, Shaheen SE, et al. (2007) Theoretical studies on conjugated phenyl-cored thiophene dendrimers for photovoltaic applications. J Am Chem Soc 129: 14257-14270.

46. Lin B, Cheng CP, You ZQ, Hsu CP (2005) Charge transport properties of tris(8-hydroxyquinolinato)aluminum(III): why it is an electron transporter. J Am Chem Soc 127: 66-67.

47. Gruhn NE, da Silva Filho DA, Bill TG, Malagoli M, Coropceanu V, et al. (2002) The vibrational reorganization energy in pentacene: molecular influences on charge transport. J Am Chem Soc 124: 7918-7919.